



**HAL**  
open science

## Cardiac radioablation for ventricular tachycardia: Which approach for incorporating cardiorespiratory motions into the planning target volume?

Julien Bellec, Louis Rigal, Aurélien Hervouin, Raphaël Martins, Mathieu Lederlin, Nicolas Jaksic, Joël Castelli, Karim Benali, Renaud de Crevoisier,  
Antoine Simon

### ► To cite this version:

Julien Bellec, Louis Rigal, Aurélien Hervouin, Raphaël Martins, Mathieu Lederlin, et al.. Cardiac radioablation for ventricular tachycardia: Which approach for incorporating cardiorespiratory motions into the planning target volume?. *Physica Medica European Journal of Medical Physics*, 2022, 95, pp.16-24. 10.1016/j.ejmp.2022.01.004 . hal-03554463

**HAL Id: hal-03554463**

**<https://hal.science/hal-03554463>**

Submitted on 23 Jun 2022

**HAL** is a multi-disciplinary open access archive for the deposit and dissemination of scientific research documents, whether they are published or not. The documents may come from teaching and research institutions in France or abroad, or from public or private research centers.

L'archive ouverte pluridisciplinaire **HAL**, est destinée au dépôt et à la diffusion de documents scientifiques de niveau recherche, publiés ou non, émanant des établissements d'enseignement et de recherche français ou étrangers, des laboratoires publics ou privés.



Distributed under a Creative Commons Attribution - NonCommercial 4.0 International License

## Cardiac radioablation for ventricular tachycardia: Which approach for incorporating cardiorespiratory motions into the planning target volume?

Julien Bellec\*<sup>1</sup>, Louis Rigal\*<sup>2</sup>, Aurélien Hervouin<sup>1</sup>, Raphaël Martins<sup>2</sup>, Mathieu Lederlin<sup>2</sup>, Nicolas Jaksic<sup>3</sup>, Joël Castelli<sup>2</sup>, Karim Benali<sup>4,5</sup>, Renaud de Crevoisier<sup>2</sup>, Antoine Simon<sup>2</sup>

\* *Julien Bellec and Louis Rigal equally contributed to this paper*

### Abstract

**Purpose:** To evaluate different approaches for generating a cardiorespiratory ITV for cardiac radioablation.

**Methods:** Four patients with ventricular tachycardia were included in this study. For each patient, cardiac-gated and respiration-correlated 4D-CT scans were acquired. The cardiorespiratory ITV was defined using registrations of the cardiac and respiratory 4D-CT images. Five different approaches, which differed in the number of incorporated cardiac phases (1, 2, 10, or 1 with a fixed 3 mm margin (FM) expansion) and respiratory phases (2 or 10), were evaluated. For each approach, a VMAT treatment plan was simulated. Target coverage (TC) and spill were evaluated geometrically and dosimetrically for each approach.

**Results:** When employing one cardiac phase, the TC did not exceed 85%. Using the two extreme phases of the cardiac and respiratory cycles resulted in a geometric TC < 88% for two patients, with a dosimetric TC of 83% for one patient. An acceptable TC for all patients (geometric TC > 89%, dosimetric TC > 92%) was only achieved when combining 10 respiratory phases with either 2 or 10 cardiac phases or a single cardiac phase with FM. The use of a single cardiac phase with FM combined with 10 respiratory phases lead to a mean geometric and dosimetric spill of 43% and 35%, respectively.

---

<sup>1</sup> Department of Medical Physics, CLCC Eugène Marquis, F-35042 Rennes, France

<sup>2</sup> Univ Rennes, CHU Rennes, CLCC Eugène Marquis, Inserm, LTSI – UMR 1099, F-35000 Rennes, France

<sup>3</sup> Department of Radiation Oncology, CLCC Eugène Marquis, F-35042 Rennes, France

<sup>4</sup> Saint-Etienne University Hospital, Department of Cardiology, Saint-Priest-En-Jarez, F-42270, France

<sup>5</sup> Inserm-IADI, UMR 947, Vandœuvre lès-Nancy, F-54500, France

**Conclusion:** For cardiac radioablation, the use of two extreme cardiac phases combined with 10 respiratory phases is a robust approach to generate a cardiorespiratory ITV. The use of a single cardiac phase with or without fixed margin expansion is not recommended based on this study.

Keywords: Cardiac radioablation, ventricular tachycardia, motion management, ITV, CT-4D

## 1. Introduction

Cardiac radioablation (CR) has recently emerged as a therapeutic option to treat cardiac arrhythmias in patients with recurrent ventricular tachycardia (VT) after being treated using the standard workflow, including antiarrhythmic drugs and/or catheter radiofrequency ablation [1]. CR involves the delivery of a single 25 Gy dose to the cardiac substrate identified as the source of abnormal electrical propagation. Both C-arm linear accelerators (linacs) (Elekta and Varian platforms) and the CyberKnife robotic system (Accuray), which are typically implemented for stereotactic body radiotherapy (SBRT), have been considered for CR of VT [2,3].

One of the main technical challenges when implementing CR is the management of target motion induced by both heart beats and respiration. It has been shown in the literature that both cardiac and respiratory motions impact target position. Prusator et al. [4] reported mean amplitudes of cardiac target displacements caused by heart contraction of 3.4 mm left/right, 4.3 mm anterior/posterior, and 4.1 mm superior/inferior. Mean target displacements induced by respiration have been reported as 3.9 mm left/right, 4.1 mm anterior/posterior, and 4.7 mm superior/inferior. Additionally, these motions are highly patient-specific, depending on the location of the target in the heart and the respiration amplitude [4,5]. The main target motion management technique used in CR, especially when using a C-arm linear accelerator, is the generation of a cardiorespiratory internal target volume (ITV) based on cardiac-gated and/or respiration-gated four-dimensional computed-tomography (4D-CT) scans [3]. A cardiorespiratory ITV is defined as encompassing all positions of the target during heartbeats and respiration. However, there is no consensus on the optimal approach for its generation, with the methods considered in the literature generally only weakly described. Therefore, a clinically feasible approach for defining the cardiorespiratory ITV must be defined and validated. It should answer several questions that remain open. For example, should cardiac motion be specifically integrated into

the definition of cardiorespiratory ITV? What is the efficiency of a fixed-margin-based approach versus a personalized strategy? How can cardiac and respiratory 4D-CT scans be utilized and combined? This study sought to answer these questions. Hence, we evaluated different methods of defining the cardiorespiratory ITV based on cardiac-gated and respiration-gated 4D-CT scans, from the use of fixed margins to the utilization of the full dynamic sequences. To identify the most appropriate method, the proposed approaches were evaluated and compared using both geometric and dosimetric criteria.

## **2. Materials and methods**

### *2.1. 4D imaging description*

CT images were acquired from four patients who were candidates to receive cardiac SBRT for VT. For each patient, two CT sequences were acquired: a cardiac-gated 4D-CT scan [6] and a respiratory-gated 4D-CT scan. Depending on the patient, other imaging modalities were used to delineate the clinical target volume (CTV) (TEP and/or electro-anatomical mapping).

Cardiac CT scan acquisition was performed with breath holding at submaximal inspiration, after thorough training, on a Somaton Force 384 slice CT scanner (Siemens, Munich, Germany). The reconstruction field of view was adjusted to include the entire heart, and intravenous contrast was administered to visualize the cardiac cavities. To demonstrate the entire cardiac cycle, 10 CT images sets were retrospectively reconstructed based on the electrocardiogram (ECG) with a slice thickness of 0.5 mm. Additionally, an average cardiac CT dataset was reconstructed from the 10 phases of the cardiac 4D-CT scan.

The respiratory-gated 4D-CT images were acquired under free breathing on a Confidence 24-slice CT scanner (Siemens, Munich, Germany). A sentinel surface-guided system (C-RAD, Stockholm, Sweden) was used to record respiratory signals during image acquisition and binning. A total of 10 respiratory phase-sorted CT datasets were retrospectively reconstructed with a slice thickness of 2 mm. Additionally, an average respiratory CT dataset was reconstructed from the 10 phases of the respiratory 4D-CT scan.

Cardiac 4D-CT datasets, respiratory 4D-CT datasets, and other useful imaging datasets, if available, were all imported into a MIM platform v7.0 (MIM Software Inc, Cleveland OH, USA), which was used for target volume definition.

## 2.2. Cardiorespiratory ITV creation

For each patient, five different methods were employed to generate the cardiorespiratory ITV. Figure 1 illustrates the concept of the methods. All were decomposed in two steps: first, the cardiac motions were integrated to define a cardiac ITV using the cardiac 4D-CT information, and then the respiratory motions were incorporated through respiratory 4D-CT images to generate the final cardiorespiratory ITV. The five evaluated methods differed in the number of phases incorporated from the 4D-CT scans to characterize cardiac and respiratory motions as defined below:

- *Card\_10ph/resp\_10ph*: It utilizes all the available images, i.e., combined all 10 cardiac phases with all 10 respiratory phases to generate the cardiorespiratory ITV.
- *Card\_2ph/resp\_10ph*: It generates cardiorespiratory ITV using the two extreme phases of the cardiac cycle combined with all 10 respiratory phases.
- *Card\_1ph/resp\_10ph*: It simulates a commonly used approach that consists of evaluating the combined cardiorespiratory target motions using only the respiratory 4D-CT scan [1,7–10]. The assumption behind this approach is to consider that respiratory-phase-binned 4D-CT images are blurred by cardiac contraction and thus implicitly integrate cardiac motion information.
- *Card\_FM/resp\_10ph*: It simulates the use of fixed margins to compensate cardiac motions. An isotropic 3 mm margin has been used since it was reported in a study where patients were treated using a Cyberknife [11]. In our study, the resulting volume was propagated over the 10 respiratory phases for the integration of respiratory motions.
- *Card\_2ph/resp\_2ph*: It integrates cardiorespiratory motions using only the two extreme phases of both the cardiac and respiratory cycles.

The practical flowchart for generating cardiorespiratory ITV with the *card\_10ph/resp\_10ph* method is described in detail in Figure 2. The creation of the cardiorespiratory ITV was divided into three main steps:

- First, the arrhythmogenic substrate (defined as the CTV in this study for consistency with conventional radiation oncology terminology) was delineated by a cardiologist on the end-of-diastole CT dataset. Delineation of the end-of-diastole CTV was performed manually after aligning image planes with the three main axes of the heart [12].
- Next, the end-of-diastole CTV was propagated from the end-of-diastole phase to the nine other cardiac phases through diffeomorphic demons deformable image registration (DIR) [13]. A cardiac ITV was generated by merging the CTV from different numbers of phases, based on the method being considered. For the *card\_10ph/resp\_10ph* method, the cardiac ITV was created by the union of all 10 cardiac phase-related CTVs. For the *card\_2ph/resp\_10ph* and *card\_2ph/resp\_2ph* methods, the cardiac ITV was defined as the union of the end-diastole CTV and the end-of-systole propagated CTV. For these three approaches, the resulting cardiac ITV was transferred to the average cardiac 4D-CT dataset. For the *card\_1ph/resp\_10ph*, no cardiac ITV was used, and only the end-of-diastole CTV was considered from the cardiac 4D-CT information. With the *card\_FM/resp\_10ph* method, a non-patient-specific cardiac ITV was defined as the end-of-diastole CTV, plus a fixed 3 mm isotropic margin expansion.
- Finally, the cardiorespiratory ITV with combined cardiac and respiratory target motions was generated by incorporating the respiratory 4D-CT scans. For this purpose, the cardiac ITV (or the end-of-diastole CTV for the *card\_1ph/resp\_10ph* method) was propagated on the 10 respiratory phases using a registration of the average cardiac 4D-CT image (or the end-of-diastole phase CT for the *card\_1ph/resp\_10ph* and *card\_FM/resp\_10ph* methods) to each of the 10 phases of the respiratory 4D-CT scan. The registration process was performed as follows. Initially, automatic rigid registration based on intensity values was performed on the full volume of both images to roughly align the structures. Then, a second automatic rigid registration was performed on a volume of interest encompassing the whole heart only, to adjust the heart-to-heart registration while ignoring other high-intensity structures. Each

registration result was visually inspected and validated by a radiation oncologist and a cardiologist. Using the resulting transformation matrices, cardiac ITV (or end-of-diastole CTV for the *card\_1ph/resp\_10ph* method) were propagated to all 10 phases of the respiratory 4D-CT scan and finally merged to generate the cardiorespiratory ITV.

The resulting cardiorespiratory ITVs from the five methods were finally associated with the average respiratory 4D-CT dataset, which is the commonly used 4D-CT dataset for treatment planning and dose calculation when implementing an ITV-based strategy [14,15].

### 2.3. Geometric evaluation

For evaluation purposes, the cardiorespiratory ITV from the *card\_10ph/resp\_10ph* method was considered as the reference as it incorporates all available information from the cardiac and respiratory 4D-CT scans. For each method, the geometric target coverage ( $C_g$ ) and geometric spill ( $S_g$ ) were quantified. The concepts of coverage and spill are illustrated in Figure 3. Here,  $C_g$  refers to the proportion of the evaluated cardiorespiratory ITV overlapping the reference cardiorespiratory ITV (i.e., generated with the *card\_10ph/resp\_10ph* method), and  $S_g$  refers to the proportion of the evaluated ITV that did not overlap with the reference cardiorespiratory ITV.

### 2.4. Dosimetric evaluation

For each patient and each method, a planning target volume (PTV) was generated using an isotropic 3 mm margin around the cardiorespiratory ITV. The 3 mm expansion was chosen based on the previous work of our group, which demonstrated that a 3 mm margin ensured correct target coverage for lung targets when using an ITV-based strategy in a Carm linac with advanced 4D-CBCT-based image guidance [16]. A volumetric modulated arc therapy (VMAT) treatment plan was simulated using a v9.10 treatment planning system (Philips Radiation Oncology Systems, Milpitas, USA) with a VersaHD linac (Elekta, Crawley, UK). The treatment plans were created using two coplanar arcs of  $358^\circ$  with a 6 MV flattening filter free (FFF) photon beam. A dose of 25 Gy was prescribed to the

PTV in a single fraction. For each treatment plan, the goal was to cover at least 95% of the PTV with at least 95% of the prescription dose ( $PTV_{D95\%} \geq 23.75$  Gy) while respecting target and organ-at-risk dose constraints from the RAVENTA trial [17]. Treatment plans were optimized to place hotspots within the ITV (with a maximum allowed dose of 35 Gy). Tuning structures (3, 15, and 40 mm rings) were used to increase the dose fall-off. Over all the patients and PTV approaches, treatment plans have been optimized to achieve a PTV coverage equal or higher than 95% ( $V_{PTV, 23.75\text{ Gy}} \geq 95\%$ ). To avoid any biases, a PTV coverage normalization was performed, for each patient, over the different PTV approaches. In practice, all patient-specific treatment plans were normalized after the optimization process in order to achieve the same PTV coverage with a coverage variation within  $\pm 0.5\%$  over all approaches.

Each method was evaluated dosimetrically by calculating the dosimetric coverage ( $C_d$ ) and dosimetric spill ( $S_d$ ) indices following the definitions described in Figure 4. Here,  $C_d$  refers to the proportion of the prescription isodose volume overlapping the reference PTV, and  $S_d$  refers to the proportion of the prescription isodose volume that did not overlap with the reference PTV. The prescription isodose volume was considered 95% of the prescribed dose (i.e. 23.75 Gy). The isodose value covering 95% of the reference PTV ( $D95\%$ ) and the median dose ( $D50\%$ ) to the heart volume minus the reference PTV were also reported for each method.

### 3. Results

The data of the four patients enrolled for CR for VT in our institution were processed using different approaches.

#### 3.1. Geometric impact of cardiorespiratory motions on the target volume

Figure 5 illustrates the CTV, cardiac ITV, and cardiorespiratory ITV obtained using the *card\_10ph/resp\_10ph* method. The CTV differed among patients, both in terms of localization (septal, infero-basal, infero-lateral, and inferior, respectively, for patients 1–4) and volume (CTV ranging from 15 cc to 78 cc).



Compared to the CTV, when incorporating all cardiac CT images, the cardiac ITV increased by a proportion of 39% to 75%. When incorporating respiratory motion using all respiratory CT images, the ITV was increased between 27% and 100%. In total, the generation of the cardiorespiratory ITV using all cardiac and respiratory 4D-CT images increased the target volume by between 76% (patient 1) and 249% (patient 4).

### 3.2. Geometric evaluation

Figure 6 presents the values of  $C_g$  and  $S_g$  obtained for the cardiorespiratory ITVs of the evaluated methods, with respect to the reference ITV (i.e., the ITV obtained by the *card\_10ph/resp\_10ph* method). The values obtained by this method are considered, by definition, as being optimal ( $C_g = 100\%$ ,  $S_g = 0\%$ ). The highest  $C_g$  obtained by another approach was the *card\_FM/resp\_10ph* method. However, this method resulted in large  $S_g$  values, ranging from 34% (patient 3) to 52% (Patient 1). The *card\_2ph/resp\_10ph* method produced a  $C_g$  larger than 89% for all patients. The  $C_g$  obtained by the *card\_1ph/resp\_10ph* method ranged from 67% and 85%, and the values obtained by the *card\_2ph/resp\_2ph* method were between 72% and 88%. These methods produced a  $S_g$  value equal to 0%, except for *card\_1ph/resp\_10ph* of patient 2, with 4%.

### 3.3. Dosimetric evaluation

Figure 7 reports the volumes of the PTV generated using the five evaluated methods. As the *card\_10ph/resp\_10ph* method can be considered as the most robust approach for defining the cardiorespiratory ITV, the resulting PTV was considered as the reference PTV. Table 1 reports the variation of PTV volumes as a function of the cardiorespiratory ITV approach implemented. By comparison, the method using fixed margins for cardiac motion management (i.e., *card\_FM/resp\_10ph* method) systematically overestimated the PTV by 20% (patient 3) to 37% (patient 1). Conversely, the exclusion of cardiac motion using the *card\_1ph/resp\_10ph* method produced the largest underestimation of PTV, with a mean underestimation of 18%. Meanwhile, the *card\_2ph/resp\_10ph* and *card\_2h/resp\_2ph* methods produced mean underestimations of 7% and 15%, respectively.

The PTV coverage ( $V_{PTV, 23.75 \text{ Gy}}$ ) over all evaluated approaches ranged from 96.8% to 97.2%, from 95.4% to 95.6%, from 95.0% to 95.5% and from 96.0% to 96.2% for patients 1, 2, 3 and 4, respectively. The dose distribution optimized on the PTV created with the *card\_10ph/resp\_10ph* method is illustrated in Figure 8 for the four patients.

Figure 9 shows the  $C_d$  and  $S_d$  values obtained by the five methods with respect to the reference PTV. Further, the D95% of the target and D50% of the heart minus the PTV were reported.

The highest  $C_d$  (Fig. 9a) was obtained using the *card\_FM/resp\_10ph* method, with a mean  $C_d$  of 99%. In decreasing order of performance, the methods *card\_10ph/resp\_10ph*, *card\_2ph/resp\_10ph*, *card\_2ph/resp\_2ph*, and *card\_1ph/resp\_10ph* produced mean  $C_d$  values of 96%, 93%, 91%, and 89%, respectively. This was confirmed using the D95% of the reference PTV, with the highest values for the *card\_FM/resp\_10ph* method producing a mean value of 26.3 Gy (higher than the prescribed dose of 25 Gy). The lowest values were obtained by using the *card\_1ph/resp\_10ph* method with 21.5 Gy for patient 4 (86% of the prescribed dose).

For dosimetric spill, the worst results (i.e., the highest  $S_d$  values) were obtained by the *card\_FM/resp\_10ph* method, with a mean value of 35%, and a maximum of 41%. In contrast, the lowest  $S_d$  was obtained by the *card\_2ph/resp\_2ph* and *card\_1ph/Resp\_10ph* methods, with mean  $S_d$  values of 12%, followed by the *card\_2ph/resp\_10ph* and *card\_10ph/resp\_10ph* methods, with mean  $S_d$  values of 15% and 19%, respectively. The D50% delivered to the heart minus PTV were all below the recommended 5 Gy value, except for the *card\_FM/resp\_10ph* method for patients 1 and 2.

#### **4. Discussion**

Due to the high delivered dose (25 Gy in a single fraction), CR of VT requires optimal definition of the PTV to obtain the expected therapeutic ratio, which involves the accurate incorporation of both cardiac-induced and respiratory-induced target motion. However, there is no consensus on the ideal management of these motions. In this study, we compared the geometric and dosimetric impacts of different methods used to generate a cardiorespiratory ITV by utilizing cardiac and respiratory 4D-CT scans. The variability among all considered indicators for these patients must be noted. Target

volumes and localizations and the impact of cardiac and respiratory motions, such as coverage of target and organs at risk, varied significantly. To date, CTVs ranging from 3.5 to 89.0 mL have been reported [3]. The volumes obtained in our study were included in this range (between 15 and 78 mL). For patient 2, a larger CTV volume was observed compared to other patients since the CTV was delineated using only CT and PET imaging because of a contraindication to electro-anatomical exploration.

When using conventional C-arm linacs, different approaches have been reported to incorporate the cardiorespiratory motion uncertainties into the PTV [1,9,10,18]. Most approaches rely on a passive motion-encompassing technique using an ITV-based strategy. Some teams assessed combined cardiorespiratory motions on the sole respiration-correlated 4D-CT scan [1,7–10], while others employed ECG-gated cardiac 4D-CT scans to isolate cardiac motion [18–20]. When using a CyberKnife system, an active respiratory compensation technique was systematically implemented [21]; thus, only cardiac ITV was considered [19,20,22,23]. Gianni et al. [11] used fixed margins to account for cardiac motion. Other teams did not explicitly take into account the cardiac target motion when defining the planning target volume [24,25].

By considering all phases of both CT scans, we first demonstrated that both cardiac and respiratory motions have an impact on the target volume. Cardiac motion alone produced an increase in target volume up to 75%, while respiratory motion alone could double the target volume. When combining both motions, the increase in the target volume reached up to 249%. When implementing an ITV-based strategy, the integration of cardiorespiratory motion into the PTV during treatment planning is thus considered essential to ensure optimal treatment delivery.

In this study, we propose a workflow (*card\_10ph/resp\_10ph*) to generate a patient-specific cardiorespiratory ITV using all phases of both cardiac and respiratory CT scans. The workflow is based on the definition of a cardiac ITV from all phases of the cardiac 4D-CT scan using deformable image registration, and its propagation to all phases of the respiratory 4D-CT scan. However, its implementation is complex. In the absence of validated deformable registration tools enabling the propagation of the CTV from one phase of the cardiac CT scan to the others, the delineation of each

phase may be required, which is time consuming and prone to variability. Thus, simplified approaches based on a subset of images would be clinically useful.

To define the cardiorespiratory ITV, methods based on the incorporation of a unique cardiac phase, with or without margins (*card\_FM/resp\_10ph* and *card\_1ph/resp\_10ph*), were not able to generate adequate target volumes for all patients. For example, the *card\_1ph/resp\_10ph* method resulted in geometric coverage  $C_g$  and dosimetric coverage  $C_d$  values for patient 1 of only 75% and 84%, respectively, which cannot be considered acceptable. The addition of a fixed 3 mm margin to the CTV improved target coverage for all patients, although it also increased the size of the PTV, and consequently the prescription isodose volume that spilled outside the target volume. Thus, the surrounding organs were unnecessarily exposed to risk. Other margin values may be considered, however, since the dynamics are highly patient specific, no unique value would be optimal for all the patients. The high spill phenomenon observed while using fixed margins is amplified when the shape of the target is close to a “C”, which happens frequently considering the conical shape of the left ventricle (e.g. for patient 2). In this study, we evaluated the utilization of the two extreme phases of both CT scans, that is, end-of-diastole and end-of-systole for the cardiac CT scan, and end-of-inspiration and end-of-expiration for the respiratory CT scan. The method based on the two extreme phases for both CT scans (*card\_2ph/resp\_2ph*) did not produce adequate geometric and dosimetric target coverage for all patients (e.g., patient 1 produced a geometric coverage  $C_g$  of 74% and a dosimetric coverage of 83%). In contrast, utilizing the two extreme cardiac phases and all respiratory phases (*card\_2ph/resp\_10ph*) correctly characterized the cardiorespiratory motion, with a geometric coverage  $C_g$  ranging from 89% to 94%, leading to a clinically acceptable dosimetric target coverage,  $C_d$ , for all patients (ranging from 92% to 95%). All these approaches except the *card\_FM/resp\_10ph* method were, by definition, smaller than the reference approach (*card\_10ph/resp\_10ph*), thus resulting in geometric spill values equal or close to 0. The non-zero geometrical spill values corresponded to a registration between cardiac and respiratory CTs based on another image than the reference approach. Indeed, if the methods based on a dynamic cardiac CT exploited the average CT image, the method *card\_1ph/resp\_10ph* exploited the registration of the end-of-diastole phase, thus potentially leading to a difference in terms of resulting geometrical transform. Concerning the

dosimetric indices, the ranking of the different methods was confirmed by the D95% index, yet it was important to note that no method presented here resulted in a D95% that was below 20Gy. The median dose to heart confirms the spill induced by *card\_FM/resp\_10ph*. It should also be noted that, in the context of CR for VT, the balance between efficacy (represented by the coverage in this study) and safety (represented by the spill) is an open question, especially because CR is still considered a last resort treatment for patients for whom standard treatments have failed.

This study demonstrates that using a single static cardiac CT scan combined with a respiration-correlated 4D-CT scan is not a sufficiently robust approach to define the cardiorespiratory ITV. The method *card\_2ph/resp\_10ph* may be considered an acceptable compromise in terms of accuracy and clinical feasibility for incorporating cardiorespiratory motions into the target volume. It may be reasonable to manually delineate the target on the two cardiac phases corresponding to the end-of-diastole and end-of-systole. Moreover, the incorporation of all respiratory phases can be considered clinical routine as it is implemented in the context of lung SBRT [14,15].

The main limitation of this study is the small patient cohort, which is due to the treatment of VT by SBRT still being an emerging technique that is only applied to a quite limited number of patients fitting specific criteria. Some uncertainties were not considered in the study, especially those related to the delineation of the target and the registration process. However, as all methods that were compared used the same delineations and registration method, these uncertainties should not have an impact on the conclusions drawn. Other imaging modalities to integrate cardiac motion may have been considered, such as echography [22,26]. Other methods to incorporate cardiorespiratory motions into the PTV may also have been considered such as probabilistic approaches as the mid-ventilation concept [27,28]. The evaluation of a probabilistic approach in the context of CR would deserve further studies as it would require specific metrics estimating the target coverage over time. The impact on target delineation of the breath holding method when acquiring the cardiac CT scan may also be studied, since the shape of the left ventricle may be influenced by the respiration phase [29]. In addition, the development of a dynamic anthropomorphic phantom would be a useful tool to simulate and evaluate the different approaches used for the management of cardiorespiratory motion in CR [30]. Finally, all treatment plans were generated by considering treatment on a C-arm linac; we did not

consider the use of CyberKnife robotic systems, which is a promising modality for the treatment of tachycardia [19]. MRI-linac is another quite promising modality, owing to its ability to visualize the heart in detail during the entire treatment [25]. Methods to derive the PTV from the CTV must be designed specifically to take advantage of the target localization abilities of these treatment devices [31].

This study demonstrates that the method implemented to integrate cardiac and respiratory motions into the target volume has an important impact on the geometry of the PTV and on the dose received by the target and surrounding organs at risk. Considering that the approaches used in the literature are heterogeneous, defining standardized approaches should be considered as a priority to safely deliver cardiac SBRT.

## 5. Conclusion

Cardiac and respiratory motions induce a large increase in target volume in CR when no active motion compensation technique is implemented. These patient-specific cardiorespiratory motions should be assessed for each patient by combining information from cardiac-gated and respiratory-gated 4D-CT scans to optimize the PTV. If the incorporation of the entire 4D-CT datasets may be challenging in clinical practice, we have shown that using only two extreme cardiac phases combined with the 10 respiratory phases is a good compromise between efficiency and clinical feasibility for the generation of a cardiorespiratory ITV. The use of only a single cardiac phase with or without a fixed margin is not recommended for optimal delivery of CR. Further studies with larger patient cohorts are warranted to support this conclusion.

## REFERENCES

- [1] Cuculich PS, Schill MR, Kashani R, Mutic S, Lang A, Cooper D, et al. Noninvasive Cardiac Radiation for Ablation of Ventricular Tachycardia. *N Engl J Med* 2017;377:2325–36. <https://doi.org/10.1056/NEJMoa1613773>.
- [2] van der Ree MH, Blanck O, Limpens J, Lee CH, Balgobind BV, Dieleman EMT, et al. Cardiac radioablation—A systematic review. *Heart Rhythm* 2020;17:1381–92. <https://doi.org/10.1016/j.hrthm.2020.03.013>.
- [3] Lydiard S, Blanck O, Hugo G, O'Brien R, Keall P. A Review of Cardiac Radioablation (CR) for Arrhythmias: Procedures, Technology, and Future Opportunities. *Int J Radiat Oncol Biol Phys* 2021;109:783–800. <https://doi.org/10.1016/j.ijrobp.2020.10.036>.

- [4] Prusator MT, Samson P, Cammin J, Robinson C, Cuculich P, Knutson NC, et al. Evaluation of motion compensation methods for non-invasive cardiac radioablation of ventricular tachycardia. *Int J Radiat Oncol Biol Phys* 2021. <https://doi.org/10.1016/j.ijrobp.2021.06.035>.
- [5] Knybel L, Cvek J, Neuwirth R, Jiravsky O, Hecko J, Penhaker M, et al. Real-time measurement of ICD lead motion during stereotactic body radiotherapy of ventricular tachycardia. *Rep Pract Oncol Radiother* 2021;26:128–37. <https://doi.org/10.5603/RPOR.a2021.0020>.
- [6] Clayton B, Roobottom C, Morgan-Hughes G. Assessment of the myocardium with cardiac computed tomography. *European Heart Journal - Cardiovascular Imaging* 2014;15:603–9. <https://doi.org/10.1093/ehjci/jeu028>.
- [7] Robinson CG, Samson PP, Moore KMS, Hugo GD, Knutson N, Mutic S, et al. Phase I/II Trial of Electrophysiology-Guided Noninvasive Cardiac Radioablation for Ventricular Tachycardia. *Circulation* 2019;139:313–21. <https://doi.org/10.1161/CIRCULATIONAHA.118.038261>.
- [8] Knutson NC, Samson PP, Hugo GD, Goddu SM, Reynoso FJ, Kavanaugh JA, et al. Radiation Therapy Workflow and Dosimetric Analysis from a Phase 1/2 Trial of Noninvasive Cardiac Radioablation for Ventricular Tachycardia. *Int J Radiat Oncol Biol Phys* 2019;104:1114–23. <https://doi.org/10.1016/j.ijrobp.2019.04.005>.
- [9] Lloyd MS, Wight J, Schneider F, Hoskins M, Attia T, Escott C, et al. Clinical Experience of Stereotactic Body Radiation For Refractory Ventricular Tachycardia in Advanced Heart Failure Patients. *Heart Rhythm* 2019;S1547527119309038. <https://doi.org/10.1016/j.hrthm.2019.09.028>.
- [10] Scholz EP, Seidensaal K, Naumann P, André F, Katus HA, Debus J. Risen from the dead: Cardiac stereotactic ablative radiotherapy as last rescue in a patient with refractory ventricular fibrillation storm. *Heart Rhythm Case Reports* 2019;5:329–32. <https://doi.org/10.1016/j.hrcr.2019.03.004>.
- [11] Gianni C, Rivera D, Burkhardt JD, Pollard B, Gardner E, Maguire P, et al. Stereotactic arrhythmia radioablation for refractory scar-related ventricular tachycardia. *Heart Rhythm* 2020;17:1241–8. <https://doi.org/10.1016/j.hrthm.2020.02.036>.
- [12] Brownstein J, Afzal M, Okabe T, Harfi TT, Tong MS, Thomas E, et al. Method and Atlas to Enable Targeting for Cardiac Radioablation Employing the American Heart Association Segmented Model. *Int J Radiat Oncol Biol Phys* 2021. <https://doi.org/10.1016/j.ijrobp.2021.03.051>.
- [13] Vercauteren T, Pennec X, Perchant A, Ayache N. Diffeomorphic demons: Efficient non-parametric image registration. *NeuroImage* 2009;45:S61–72. <https://doi.org/10.1016/j.neuroimage.2008.10.040>.
- [14] Schwarz M, Cattaneo GM, Marrazzo L. Geometrical and dosimetric uncertainties in hypofractionated radiotherapy of the lung: A review. *Physica Medica* 2017;36:126–39. <https://doi.org/10.1016/j.ejmp.2017.02.011>.
- [15] Guckenberger M, Andratschke N, Dieckmann K, Hoogeman MS, Hoyer M, Hurkmans C, et al. ESTRO ACROP consensus guideline on implementation and practice of stereotactic body radiotherapy for peripherally located early stage non-small cell lung cancer. *Radiother Oncol* 2017;124:11–7. <https://doi.org/10.1016/j.radonc.2017.05.012>.
- [16] Bellec J, Arab-Ceschia F, Castelli J, Lafond C, Chajon E. ITV versus mid-ventilation for treatment planning in lung SBRT: a comparison of target coverage and PTV adequacy by using in-treatment 4D cone beam CT. *Radiation Oncology* 2020;15:54. <https://doi.org/10.1186/s13014-020-01496-5>.
- [17] Blanck O, Buergy D, Vens M, Eidinger L, Zaman A, Krug D, et al. Radiosurgery for ventricular tachycardia: preclinical and clinical evidence and study design for a German multi-center multi-platform feasibility trial (RAVENTA). *Clin Res Cardiol* 2020;109:1319–32. <https://doi.org/10.1007/s00392-020-01650-9>.
- [18] Krug D, Blanck O, Demming T, Dottermusch M, Koch K, Hirt M, et al. Stereotactic body radiotherapy for ventricular tachycardia (cardiac radiosurgery): First-in-patient treatment in Germany. *Strahlenther Onkol* 2019. <https://doi.org/10.1007/s00066-019-01530-w>.
- [19] Neuwirth R, Cvek J, Knybel L, Jiravsky O, Molenda L, Kodaj M, et al. Stereotactic radiosurgery for ablation of ventricular tachycardia. *EP Europace* 2019;21:1088–95. <https://doi.org/10.1093/europace/euz133>.
- [20] Cvek J, Neuwirth R, Knybel L, Molenda L, Otahal B, Pindor J, et al. Cardiac Radiosurgery for Malignant Ventricular Tachycardia. *Cureus* 2014. <https://doi.org/10.7759/cureus.190>.

- [21] Adler Jr JR, Chang SD, Murphy MJ, Doty J, Geis P, Hancock SL. The Cyberknife: A Frameless Robotic System for Radiosurgery. *Stereotact Funct Neurosurg* 1997;69:124–8. <https://doi.org/10.1159/000099863>.
- [22] Loo BW, Soltys SG, Wang L, Lo A, Fahimian BP, Jagaru A, et al. Stereotactic Ablative Radiotherapy for the Treatment of Refractory Cardiac Ventricular Arrhythmia. *Circ Arrhythm Electrophysiol* 2015;8:748–50. <https://doi.org/10.1161/CIRCEP.115.002765>.
- [23] Zeng L, Huang L, Tan H, Zhang H, Mei J, Shi H, et al. Stereotactic body radiation therapy for refractory ventricular tachycardia secondary to cardiac lipoma: A case report. *Pacing Clin Electrophysiol* 2019;42:1276–9. <https://doi.org/10.1111/pace.13731>.
- [24] Peichl P, Sramko M, Cvek J, Kautzner J. A case report of successful elimination of recurrent ventricular tachycardia by repeated stereotactic radiotherapy: the importance of accurate target volume delineation. *Eur Heart J Case Rep* 2020:ytaa516. <https://doi.org/10.1093/ehjcr/ytaa516>.
- [25] Mayinger M, Kovacs B, Tanadini-Lang S, Ehrbar S, Wilke L, Chamberlain M, et al. First magnetic resonance imaging-guided cardiac radioablation of sustained ventricular tachycardia. *Radiother Oncol* 2020:S0167814020300207. <https://doi.org/10.1016/j.radonc.2020.01.008>.
- [26] Jumeau R, Ozsahin M, Schwitter J, Vallet V, Duclos F, Zeverino M, et al. Rescue procedure for an electrical storm using robotic non-invasive cardiac radio-ablation. *Radiother Oncol* 2018;128:189–91. <https://doi.org/10.1016/j.radonc.2018.04.025>.
- [27] Thomas SJ, Evans BJ, Harihar L, Chantler HJ, Martin AGR, Harden SV. An evaluation of the mid-ventilation method for the planning of stereotactic lung plans. *Radiother Oncol* 2019;137:110–6. <https://doi.org/10.1016/j.radonc.2019.04.031>.
- [28] Vander Veken L, Dechambre D, Sterpin E, Souris K, Van Ooteghem G, Aldo Lee J, et al. Incorporation of tumor motion directionality in margin recipe: The directional MidP strategy. *Physica Medica* 2021;91:43–53. <https://doi.org/10.1016/j.ejmp.2021.10.010>.
- [29] Claessen G, Claus P, Delcroix M, Bogaert J, Gerche AL, Heidbuchel H. Interaction between respiration and right versus left ventricular volumes at rest and during exercise: a real-time cardiac magnetic resonance study. *American Journal of Physiology-Heart and Circulatory Physiology* 2014;306:H816–24. <https://doi.org/10.1152/ajpheart.00752.2013>.
- [30] Erdoğan T, Fidan U, Özyiğit G. Patient-specific tumor and respiratory monitoring phantom design for quality controls of stereotactic ablative body radiotherapy in lung cancer cases. *Physica Medica* 2021;90:40–9. <https://doi.org/10.1016/j.ejmp.2021.09.003>.
- [31] Dieterich S, Green O, Booth J. SBRT targets that move with respiration. *Physica Medica* 2018;56:19–24. <https://doi.org/10.1016/j.ejmp.2018.10.021>.



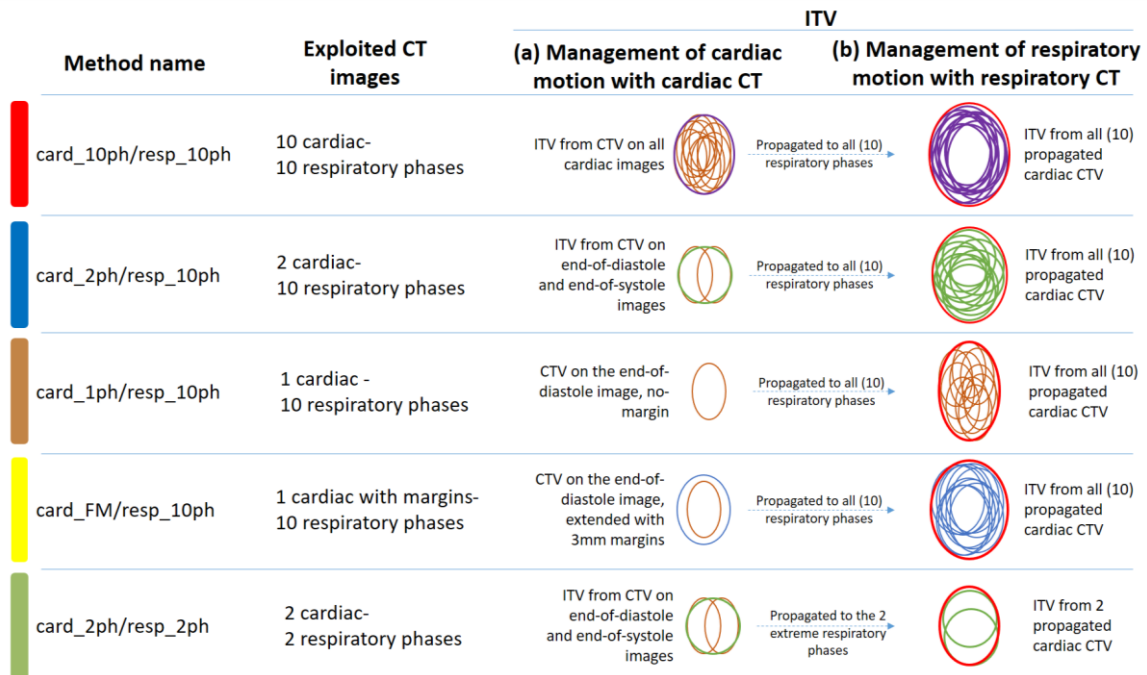


Fig 1. Approaches considered for the cardiorespiratory ITV generation.

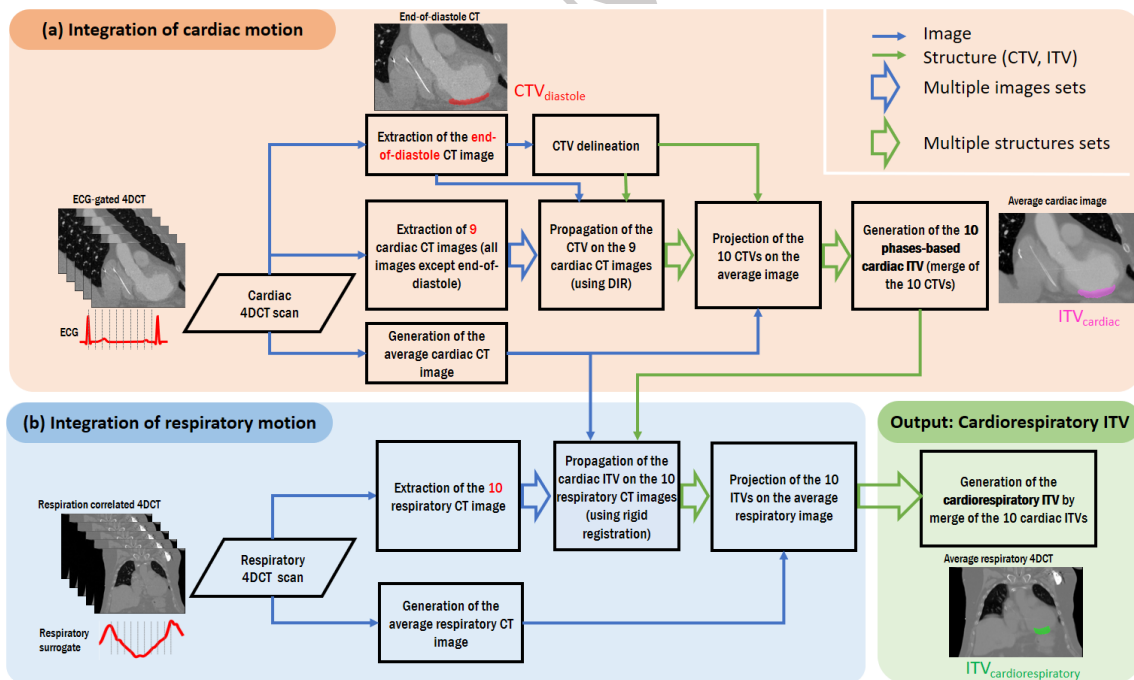


Fig 2. Reference workflow. Workflow used to generate the cardiorespiratory ITV using the card\_10ph/resp\_10ph method (i.e., the method utilizing all 10 cardiac and respiration phases). All other methods employed the same framework, differing in the number of CT images incorporated.

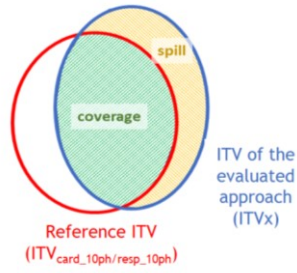


Fig 3. Illustration of geometric coverage ( $C_g$ ) and geometric spill ( $S_g$ ) concepts. By definition, for the  $ITV_{card\_10ph/resp\_10ph}$ ,  $C_g = 100\%$  and  $S_g = 0\%$ .

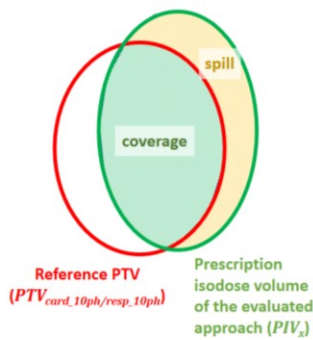


Fig 4. Illustration of dosimetric coverage ( $C_d$ ) and dosimetric spill ( $S_d$ ) concepts. The prescription isodose volume refers to the 95% of the prescribed dose (i.e. 23.75 Gy)

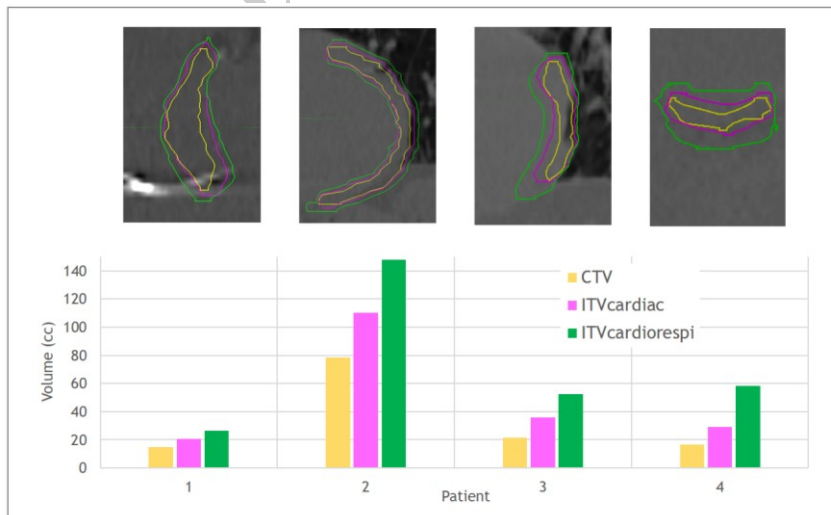


Fig 5. Volumetric contribution of cardiorespiratory motions management. CTV, cardiac ITV, and cardiorespiratory ITV volumes for the four patients generated with the exhaustive approach (*card\_10ph/resp\_10ph* method). For each patient, the upper image represents the different volumes overlaid on one respiratory CT image in a sagittal plane (not to scale).



Fig 6. Comparison of the different approaches for generating the cardiorespiratory ITV using geometric criteria. Including geometric target coverage  $C_g$  (a) and geometric spill  $S_g$  (b).

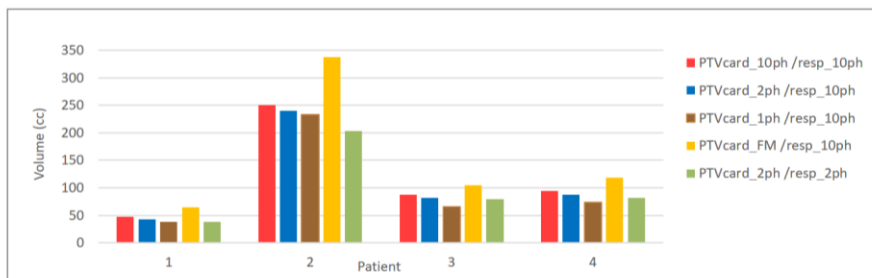


Fig 7. PTVs from the different cardiorespiratory ITV approaches.

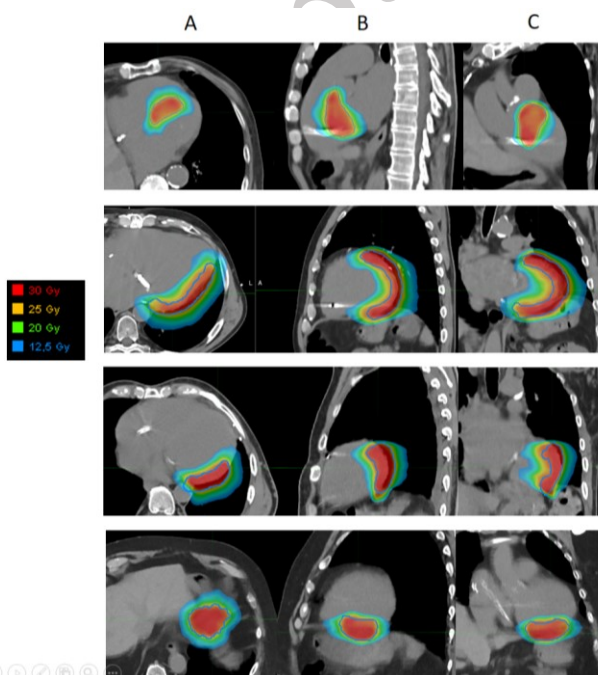


Fig 8. Planning dose distribution for the four patients. Planning average respiratory-correlated 4D-CT with overlaid PTV obtained using the *card\_10ph/resp\_10ph* method (blue line) and dose distributions in axial (A), sagittal (B), and coronal (C) planes for the four patients. Treatment plans were simulated using the VMAT coplanar dual arc technique.

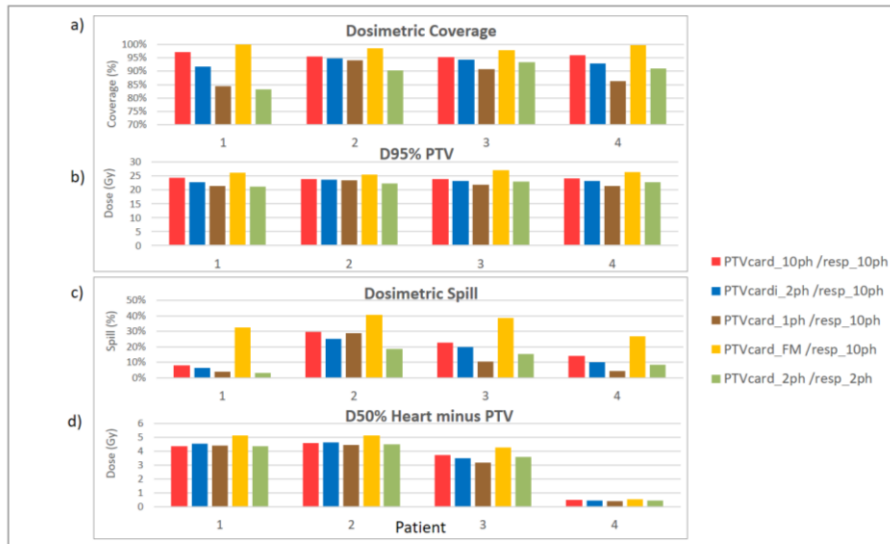


Fig 9. Dosimetric evaluation of the methods used to generate the cardiorespiratory ITVs. Each resulting 23.75 Gy isodose (95% of the prescribed dose) is compared to the PTV generated with the method utilizing all 4D-CT images (*card\_10ph/resp\_10ph* method). The comparison criteria are dosimetric target coverage  $C_d$  (a), dose received by 95% of the reference PTV (b), dosimetric spill  $S_d$  (c), and median dose (D50%) received by the heart minus the PTV (d).

Table 1. Variation of PTV volumes as a function of the cardiorespiratory ITV approach implemented

	$PTV_{card\_10ph/resp\_10ph}$	$PTV_{card\_2ph/resp\_10ph}$	$PTV_{card\_1ph/resp\_10ph}$	$PTV_{card\_FM/resp\_10ph}$	$PTV_{card\_2ph/resp\_2ph}$
Absolute PTV volume Mean (min, max) [cc]	120 (47, 250)	113 (43, 239)	103 (38, 233)	157 (65, 337)	100 (37, 202)
Relative PTV volume difference with reference to $PTV_{card\_10ph/resp\_10ph}$ Mean (min, max) [%]	-	-7% (-4%, -9%)	-18% (-7%, -25%)	+28% (+20%, +37%)	-15% (-9%, -20%)